Expert Systems with Applications 40 (2013) 4922–4933

Contents lists available at SciVerse ScienceDirect

Expert Systems with Applications

journal homepage: www.elsevier.com/locate/eswa

Multifractal scaling behavior analysis for existing dams

Huaizhi Su [a,b,*], Zhiping Wen [c], Feng Wang [d], Bowen Wei [b], Jiang Hu [d]

[a] State Key Laboratory of Hydrology-Water Resources and Hydraulic Engineering, Hohai University, Nanjing 210098, China
[b] College of Water Conservancy and Hydropower Engineering, Hohai University, Nanjing 210098, China
[c] Department of Computer Engineering, Nanjing Institute of Technology, Nanjing 211167, China
[d] National Engineering Research Center of Water Resources Efficient Utilization and Engineering Safety, Nanjing 210098, China

ARTICLE INFO

Keywords:
Dam
Long term behavior
Observation time series
Multifractal detrended fluctuation analysis

ABSTRACT

The fractal theory was used to describe long term behavior of dam structures by means of determining (mono-) fractal exponents. Many records do not exhibit a simple monofractal scaling behavior, which can be accounted for by a single scaling exponent. In this paper the multifractal detrended fluctuation analysis (MF-DFA) is employed to analyze the time series of *in situ* observed data of existing dam which intrinsically reflects its long term behavior and structural evolution law. Deformation analysis of one gravity dam is taken as an example, the multifractal characteristic of the time series is obtained. The results show that this method can reliably determine the multifractal scaling behavior of time series of existing dams. The fractal theory can be applied to predict and diagnose dam behavior.

1. Introduction

Dam and foundation can be regarded as a complex nonlinear dynamic system. Dam behavior exhibits significant spatiotemporal nonlinear characteristics under the combining influencing of external factors. For deformation, in practice, there is not just a single origin, the measured deformation signal is a result of a number of influencing factors, such as temperature, upstream and downstream water levels and physical properties of concrete. *In situ* observed time series permits effective assessment of the ongoing evolution of physical mechanism (e.g. aging and creep) in structures. In recent years mathematical monitoring models combining advanced mathematical methods and *in situ* observed time series have become widely used techniques for analyzing and identifying long term behavior of existing dams (Liu, Wu, Yang, & Hu, 2012; Loh, Chen, & Hsu, 2011; Su, Hu, & Wu, 2012).

In general, standard statistical methods are used to reveal data characteristics, assume that the observed independent and effect quantities are normally distributed. However in fact, *in situ* observed time series do not strictly follow this normal distribution. This means that the traditional deterministic or random theories cannot rightly characterize and interpret the signal time series. In addition, various independence testing methods cannot identify long-term correlate behavior. In a previous paper, monofractal exponents were obtained based on observed time series in order to give information on the inherent evolution law of a dam system (Su et al., 2012). The investigated example indicates that dam structure has self-similarity characteristics. In recent years the detrended fluctuation analysis (DFA) method has become a widely used technique for the determination of monofractal scaling properties and the detection of long-range correlations in noisy and nonstationary time series. It has successfully been applied to various fields such as DNA sequences, long-time weather records, cloud structures, geology, and solid state physics. Fractals naturally appear in many physical situations (Alvarez-Ramirez, Rodriguez, & Echeverria, 2009; Coniglio, de Arcangelis, & Herrmann, 1989; de Moura, Vieira, Irmao, & Silva, 2009; Govindan et al., 2007; Kantelhardt, Koscielny-Bunde, Rego, Havlin, & Bunde, 2001; Peng, Buldyrev, Havlin, et al., 1994). One reason to employ the DFA method is to avoid spurious detection of correlations that are artifacts of nonstationarities in the time series.

Many records do not exhibit a simple monofractal scaling behavior, but crossover (time-) scales separating regimes with different scaling exponents, e.g. long-range correlations on small scales and another type of correlations or uncorrelated behavior on larger scales (Kantelhardt et al., 2002; Telesca, Lovallo, Lopez-Moreno, & Vicente-Serrano, 2012a; Telesca, Pierini, & Scian, 2012b). A multifractal object requires many indices to characterize its scaling properties. Multifractals can be decomposed into many-possibly infinitely many sub-sets characterized by different scaling exponents. That is to say, much more information is contained in what is called a multifractal measure which is defined on a fractal can give insight about its structure or about the way it evolves. Then DFA was generalized to study the multifractal nature

* Corresponding author at: State Key Laboratory of Hydrology-Water Resources and Hydraulic Engineering, Hohai University, Nanjing 210098, China.
E-mail address: su_huaizhi@hhu.edu.cn (H. Su).

0957-4174/$ - see front matter © 2013 Elsevier Ltd. All rights reserved.
http://dx.doi.org/10.1016/j.eswa.2013.02.033

hidden in time series, termed multifractal DFA (MF-DFA) (Huang, Liu, Shi, & Zhang, 2010; Niu, Wang, Liang, Yu, & Yu, 2008; Telesca, Colangelo, Lapenna, & Macchiato, 2004; Telesca & Lovallo, 2011; Telesca, Lovallo, Hsu, & Chen, 2012). Due to complicated cases such as chemical dissolution and extreme external loads, dam behavior may change in different intervals. Dam behavior is controlled by external and internal influencing factors, such as water level and temperature. Previous research has already shown that records of these factors exhibits multifractality. Therefore, MF-DFA can be employed to investigate multifractal characteristics of time series of dam structures, and to judge different combustion status.

The main objective of this paper is to reveal the time scale effect and the nonlinear dynamic evolution law of dams using MF-DFA. The paper is organized as follows: In Section 2 the DFA method is simply described. In Section 3 the MF-DFA method is introduced and the framework for obtaining multifractals of time series of dam structures is proposed. In Section 4, the results of data analysis are present and their physical interpretations are discussed. In Section 5 comments on the current work are listed.

2. Monofractal feature identification of monitoring data sequence of dam's service behavior

Critical fluctuations, evolution or disorder can produce fractal structures which have unusual physical properties due to their scale invariance (Bernaola-Galván, Ivanov, Nunes Amaral, & Eugene Stanley, 2001; Foufoula-Georgiou, & Sapozhnikov, 2001; Kawada, Nagahama, & Nakamura, 2007). As in many physical situations, dam structure is characterized by self-similarity (Su et al., 2012). The only difference is the characteristic physical quantity accompanying in the stochastic processes.

The DFA is a method which was invented by Peng et al. in 1994 when they detected long-range correlations of DNA time series (Peng et al., 1994). The DFA can be used as a means of estimating the Hurst exponent of a time series by eliminating trends.

Let us suppose that x_i is a series of length n of dam's service behavior, and this series is of compact support. The DFA procedure consists of the following steps.

(1) Calculate the cumulative sum of the time series$\{x_t, t = 1,2,\ldots,n\}$

$$Y(i) = \sum_{t=1}^{i}(x_t - \bar{x}) \tag{1}$$

where $\bar{x} = \frac{1}{N}\sum_{t=1}^{i} x_t$.

(2) Divide the series $Y(i)$ into m non-overlapping intervals v. Each interval contains the same number of points s, where integral part is $m = [N/s]$. Since the length N of the sequence is often not an integral multiple of s. In order not to disregard the data at the end of the sequence, the same procedure is repeated from the opposite end from the $m + 1$-th interval. Thereby, $2m$ intervals are obtained altogether.

(3) Calculate the local trend for each interval v by a least-square fit of the data. $Y_s(i)$ which the time series removing the trend is denoted by shows the difference between original series and fitted values

$$Y_s(i) = Y(i) - P_v^k(i) \tag{2}$$

where $P_v^k(i)$, called k-order DFA (e.g. linear, quadratic, cubic, or higher order, conventionally called DFA1, DFA2, DFA3,...), is the fitting polynomial of in vth interval; k is the different fitting order. Since the detrending of the time series is done by the subtraction of the polynomial fits from the profile, different order DFA differ in their capability of eliminating trends in the series.

(4) Then determine the variance of each interval which has already been removed the trend

$$F^2(v,s) = \frac{1}{s}\sum_{i=1}^{s} Y_s^2[(v-1)s+i], \quad v = 1,2,\cdots,2m \tag{3}$$

(5) Average over all segments to obtain the standard DFA fluctuation function

$$F(s) = \sqrt{\frac{1}{N}\sum_{v=1}^{m} F^2(v,s)} \tag{4}$$

If time series is uncorrelated or short-term correlated, then $F(s) \sim s^{1/2}$; If time series is long-term correlated, then $F(s) \sim s^{\alpha}$, $\alpha \neq 1/2$. The significance of α which is a scaling exponent and embodies the correlation property of sequence is the same as Hurst exponent.

(6) Determine the scaling relation between the DFA $F(s)$ and the size scale s, which reads

$$\lg F(s) = \lg A + \alpha \lg s \tag{5}$$

Use the least-square regression to obtain the value of α. (Kantelhardt et al., 2002; Telesca et al., 2004)

If $\alpha = 0.5$, time series is a independent process and does not exist long-term memory.
If $0 < \alpha < 0.5$, time series is characterized by inverse sustainability and shows power-law inverse correlation.
If $0.5 < \alpha < 1$, time series is characterized by positive sustainability and shows power-law positive correlation.
If $\alpha = 1$, time series is similar to white noise.
If $\alpha > 1$, time series still shows long-range correlations but deviates slowly from power-law.
If $\alpha = 1.5$, the correlation of time series is similar to Brown noise.

Therefore, scale exponent can be used to describe "roughness" of time series. The larger the scale exponent is, the more smooth time series is.

3. Multifractal features identification of monitoring data sequence of dam's service behavior

Multifractals, as well as monofractals, are ubiquitous in natural and social sciences. Much more information is contained in what is called a multifractal measure. In the case that there exist time scales separating regimes with different scaling exponents a multitude of scaling exponents is required for a full description of the scaling behavior, and a multifractal analysis must be applied. For the measured time series of dam's service behavior, its irregularity and singularity often change with time dependent influencing factors, and internal and external environment. Time scales separating regimes with different scaling exponents on different scales can be used to better depict long term behavior of dams.

3.1. Definition of multifractal approach

Multifractal approach, which is also called fractal measure, used to express a singular set of distribution of non-uniform fractal dimension which can not be described only by a holistic characteristic scaling exponent or the growth characteristics of fractal particle at different levels which can be described by a spectral function, studies its whole fractality from system part (Barabasi, & Vicsek, 1991; Halsey, Jensen, Kadanoff, Procaccia, & Shraiman, 1986; Lau, & Ngai, 1999; Longley, & Batty, 1989). Through analyzing singularity spectrum function $f(\alpha)$ of time series, multifractal analysis quantitatively depicts the distribution on the whole set of probabilities which is caused by different local conditions or different levels in the evolution process. Therefore, multifractal analysis is also a metric for the complex, irregular and inhomogeneous degree of fractal structure.

If the continuous time series $X = \{X_t: t = 1,2,\ldots\}$ has stationary increments, and for all $t \in T$, $q \in Q$, they are satisfied as follows.

$$E(|X(t+\Delta t) - X(t)|^q) = c(q)(\Delta t)^{\tau(q)+1} \tag{6}$$

then X_t can be called multifractal process. The length of real intervals Q and T are both positive, and $0 \in T$, $[0,1] \subseteq Q$; $\tau(q)$ and $c(q)$ are the functions of Q domain; $\triangle t$ is the time increment.

The above equality describes the relationship between multifractal process moment and scale power-law. The relationships of scale power-law for different time increment $\triangle t$ are the same. That is, the scale invariance is met.

When $\tau(q)$, the scaling function, has the following properties, its process is the multifractal process.

(1) $\tau(q)$ is a convex function;
(2) If $q = 0$, all scaling functions have the same intercept, that is $\tau(0) = -1$;
(3) $\tau(q)$ is the nonlinear function of q. If $\tau(q) = qH - 1$, the corresponding stochastic process is turned into monofractal process, that is the relationship between scaling function and q is linear.
(4) If $q \to \pm\infty$, $\tau(q)$ tends to be infinite.

The definition above that depicts the fractal features of different amplitude process increments and different time points through the moment scale characteristics of increments provides evidence for studying fluctuation characteristics of measured data sequence of dam's service behavior at different time scales. The scaling functions of different q values correspond to different fluctuations. The physical meaning of multifractal process is described through two special cases as follows.

(1) If $q < 0$ and $|q| \gg 10$, bigger fluctuations tend to zero after the q-th power and almost do not work in the final results. Those smaller fluctuations play important roles and q-order moment mainly depicts the characteristics of small fluctuation at this point.
(2) If $q > 0$ and $|q| \gg 10$, smaller fluctuations almost do not work while those bigger fluctuations play important roles. q-order moment mainly depicts the characteristics of big fluctuation at this point.

Thus $\tau(q)$ values corresponding to each q can be calculated first and then test multifractal structure $\{X_t\}$ of $\tau(q)$ by detecting the nonlinear relationship between $\tau(q)$ and q.

3.2. Generalized Hurst exponent

Through studies, Hurst found that rescaled range and sequence subscript n exist changed proportion of index H, that is $R/S = K(n)^H$. Where n is the length of time increment interval, K is a constant. Based on this, generalized Hurst exponent $H(q)$ can be defined by contacting the definition of stochastic process multifractality as:

$$\{E(|X(t+\Delta t) - X(t)|^q)\}^{1/q} = c(q)(\Delta t)^{H(q)} \tag{7}$$

In the above equality, $q \neq 0$, the function $H(q)$ contains the information of generalized average change under the time increment Δt .

From the comparison of equality (6) and (7), it can be seen that the relationship between generalized Hurst exponent and scaling function $\tau(q)$ is:

$$H(q) = [\tau(q) + 1]/q \tag{8}$$

Therefore, the relationship between $\tau(q)$ and q will be got if appropriate numerical method can be found to fit out $H(q)$.

3.3. MF-DFA method

Based on the previous DFA, Kantelhardt et al. proposed a robust multifractal analysis namely MF-DFA (Coniglio et al., 1989; Govindan et al., 2007). MF-DFA method takes fluctuant average of time series in each partition interval as statistical points and determines generalized Hurst exponent depending on power-law property of fluctuation function to measure stationary and non-stationary sequence structure and fluctuation singularity. The advantages of this method are that it can find the long-range correlations of non-stationary time series. And Kantelhardt et al. demonstrated with the computer simulation that the effect using MF-DFA method to analyze multifractality for non-stationary time series was the best in all methods (Govindan et al., 2007).

The concrete steps of analyzing measured data characteristics of dam's service behavior based on MF-DFA are as follows:

(1) Cumulative deviation of time series $\{x_t,\ t = 1,2,\ldots,n\}$ of dam's prototype monitoring data is calculated as

$$Y(i) = \sum_{t=1}^{i}(x_t - \bar{x}) \tag{9}$$

where $\bar{x} = \frac{1}{N}\sum_{t=1}^{i} x_t$.

(2) Divide sequence $Y(i)$ into m non-overlapping intervals ν. Each interval contains the same number of points s, where integral part is $m = [N/s]$. Since the length of the sequence is often not an integral multiple of s. In order not to produce surplus, the same procedure is repeated from the opposite end from the $m+1$-th interval. Thereby, $2m$ intervals are obtained altogether.

(3) Fitting polynomial of the ν-th interval through a least-square fit of the data for each interval $\nu(\nu = 1,2,\ldots,2m)$ can be got as:

$$\hat{y}_\nu(i) = \hat{a}_0 + \hat{a}_1 i + \cdot + \hat{a}_k i^k, \quad i = 1,2,\ldots,s, \quad k = 1,2,\ldots \tag{10}$$

$Y_s(i)$ which the time series removing the trend is denoted by shows the difference between the original series and fitted values.

$$Y_s(i) = Y(i) - \hat{y}_\nu(i) \tag{11}$$

where $\hat{y}_\nu(i)$, called k-order MF-DFA, is the local trend function of the νth interval. k is the different fitting order. In MF-DFAk (kth order MF-DFA) trends of order k in the profile (or, equivalently, of order $k-1$ in the original series) are eliminated.

(4) Calculate the variance of each interval which has been removed the trend.

If $\nu = 1,2,\ldots,m$,

$$F^2(\nu,s) = \frac{1}{s}\sum_{i=1}^{s} Y_s^2[i] = \frac{1}{s}\sum_{i=1}^{s}(y((\nu-1)s+i) - \hat{y}_\nu(i))^2 \tag{12}$$

If $\nu = m+1, m+2,\ldots,2m$,

$$F^2(\nu,s) = \frac{1}{s}\sum_{i=1}^{s} Y_s^2[i] = \frac{1}{s}\sum_{i=1}^{s}(y((n-(\nu-1))s+i) - \hat{y}_\nu(i))^2 \tag{13}$$

Obviously, $F^2(\nu,s)$ is concerned with the fitting order. Different orders have different abilities to eliminate the trend.

(5) Average and extract a root for all variances of equal-length intervals. Then the q-order fluctuation function of the whole sequence can be obtained:

$$F_q(s) = \left\{ \frac{1}{2m} \sum_{v=1}^{2m} [F^2(v,s)]^{q/2} \right\}^{1/q} \tag{14}$$

In general, the index variable q can take any real value. For $q = 0$, the fluctuation function can be determined as below equality:

$$F_0(s) = \exp\left\{ \frac{1}{4m} \sum_{v=1}^{2m} \ln[F^2(v,s)] \right\} \tag{15}$$

For $q = 2$, it can be seen that equality (14) and (4) are the same, the standard DFA procedure is retrieved. At this point, DFA is the special form of MF-DFA.

For positive q, the segments v with large variance (i.e., large deviation from the corresponding fit) will dominate the average $F_q(s)$. Therefore, if q is positive, $h(q)$ describes the scaling behavior of the segments with large fluctuations; and generally, large fluctuations are characterized by a smaller scaling exponent $h(q)$ for multifractal time series. For negative q, the segments v with small variance will dominate the average $F_q(s)$. Thus, for negative q values, the scaling exponent $h(q)$ describes the scaling behavior of segments with small fluctuations, usually characterized by a larger scaling exponents.

Therefore, different q values have different effects on fluctuation functions.

(6) Determine the scaling exponent of fluctuation function. Varying the value of s in the range from $s_{\min} \approx 5$ to $s_{\max} \approx N/4$, and repeating the procedure described above for various scales s, $F_q(s)$ will increase with increasing s. Then analyzing log–log plots $F_q(s)$ vs. s for each value of q, the scaling behavior of the fluctuation functions can be determined. If the series xi is long-range power-law correlated, $F_q(s)$ increases for large values of s as a power-law

$$F_q(s) \sim s^{h(q)} \tag{16}$$

In general the exponent $h(q)$ will depend on q. For stationary time series, $h(2)$ is the well defined Hurst exponent H. Thus, $h(q)$ is called the generalized Hurst exponent. Monofractal time series are characterized by $h(q)$ independent of q. The different scaling of small and large fluctuations will yield a significant dependence of $h(q)$ on q.

The above equality can be also expressed as $F_q(s) = As^{h(q)}$. Take logarithm for the both sides of the equality

$$\ln(F_q(s)) = \ln A + H(q)\ln(s) \tag{17}$$

A corresponding fluctuation function value $F_q(s)$ can be obtained for each partition length s; different $F_q(s)$ can be got by using different constant s. By using the least square method to make linear regression for the above equality, slope estimated value obtained is q-order generalized Hurst exponent $h(q)$.

(a) Downstream view of the dam

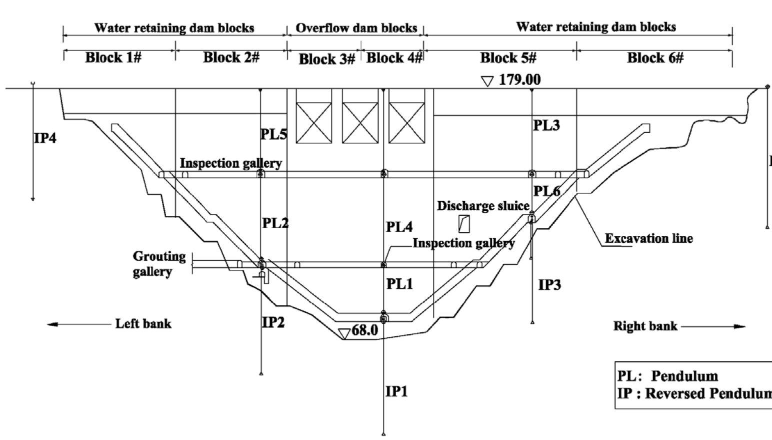

(b) Layout of observation suspended and reversed pendulums

Fig. 1. Downstream view of the dam and layout of its observation suspended pendulums.

Generalized Hurst exponent $h(q)$ has the significance of scaling exponent of DFA, but $h(q)$ is concerned with q. Time series is monofractal if $h(q)$ has nothing with q and time series is multifractal if $h(q)$ is a function of q.

(7) $h(q)$ which is obtained through MF-DFA is related to Renyi exponent $\tau(q)$, that is

$$\tau(q) = qh(q) - 1 \tag{18}$$

(8) Multifractal spectrum $f(\alpha)$ which is used to describe multifractal time series can be obtained from the below equality:

$$\alpha = h(q) + qh'(q) \tag{19}$$

$$f(\alpha) = q[\alpha - h(q)] + 1 \tag{20}$$

The shape and extension of $f(\alpha)$-curve contains significant information about the distribution characteristics of the examined data set.

4. Analysis of an engineering example

A hydropower station (shown in Fig. 1), located in southeast China, is mainly for power generation with consideration of flood control, navigation, aquaculture and other comprehensive benefits. Its main body is roller compacted concrete gravity dam which has a maximum height of 113.0 m, the crest length of 308.5 m and the elevation of 179.0 m. This dam consists of 10 blocks and numbered 1#–6# from left bank to right bank. Blocks 3 and 4 are overflow structures, others are water retaining structures. The reservoir's normal water level is 173.0 m, regulating storage is 1.12 billion m^3. To monitor long term dam behavior, deformation observation system composed of collimating lines, tension wire alignments and pendulums (as shown in Fig. 1(b)) was installed.

Typical suspended pendulums, namely PL3, PL4 and PL5 are selected to investigate monofractal features and multifractal features of the dam global behavior. In detail, the time series of horizontal displacements measured by PL4 is used to identify monofractal

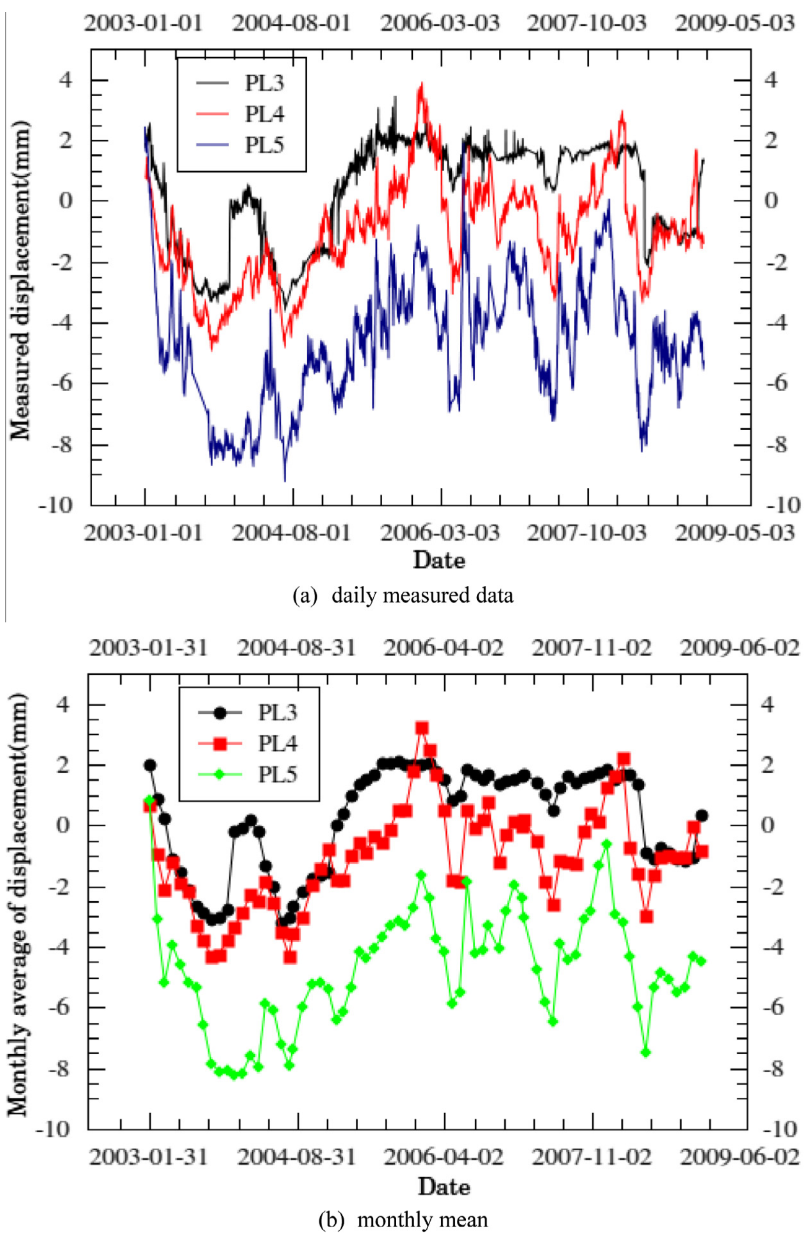

Fig. 2. Process lines of measured data of Suspended Pendulums PL3∼5 (Y direction).

features and multifractal features, and all three time series of horizontal displacements from January 1, 2003 to December 31, 2008 (N~1959, 2014 and 1967 respectively) of these suspended pendulums are used to compare corresponding behavior of Blocks3#~5#. For the convenience of result analysis, assume that downstream displacement is positive and upstream displacement is negative. Fig. 2(a) and (b) respectively show the daily measured and monthly mean time series of observed horizontal displacements (Y direction) of these suspended pendulums, According to Fig. 2, it is observed that all three time series fluctuate with the seasons with small as well as large fluctuations among different years, and obviously show the similar global trend namely small positive development. Meanwhile, to a certain extent, small differences exist among fluctuation amplitudes of these time series. Therefore, the multifractal structure is employed to reflect important properties of the deformation evolution of various dam blocks to obtain the global behavior.

4.1. Monofractal identification of dam's displacement sequence

DFA method is used to analyze displacement series of suspended pendulum of Y direction. For very large scales, the fluctuation function Fs becomes statistically unreliable because the number of segments N for the averaging procedure in Eq. (14) becomes very small. For the maximum scale, $s = N$, the fluctuation function Fs is independent of q. Based on this, the interval length of $S_{\max} \approx N/4$ and $S_{\min} \approx 5$ are generally selected. Thus, the range of s is selected from 6 to $N/4$ depending on the length of the time series.

The DFA is respectively employed to time series of daily obaservation ($N = 2014$) and monthly mean ($N = 72$) measured by PL4. Results for MF-DFA1 to MF-DFA4 are compared to detect effects of order on multifractal scaling exponents. The DFA fluctuation functions Fs of time series of monthly mean are shown versus the scale s in log–log plots for four orders in Fig. 3, and that of daily

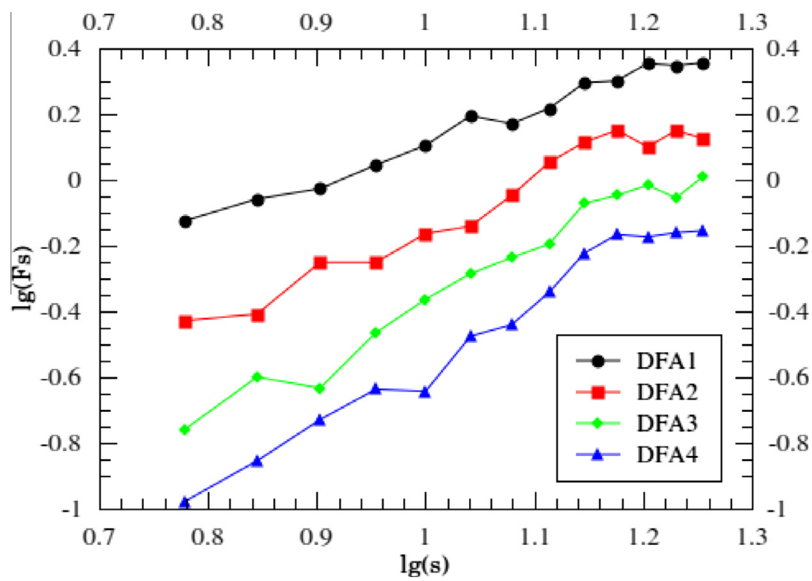

Fig. 3. Analysis results of the monthly mean for measured data of Suspended Pendulum PL4 (Y direction) by DFA.

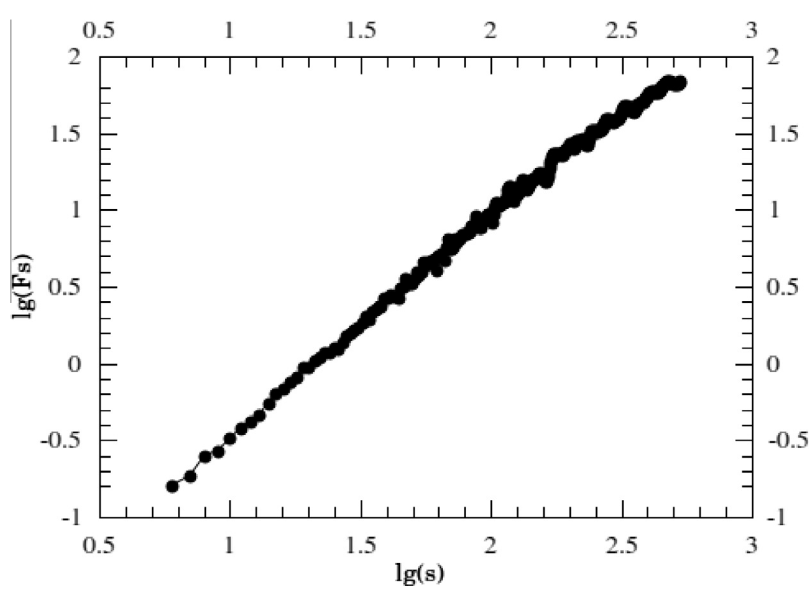

Fig. 4. Analysis results of the daily measured data of Suspended Pendulum PL4 (Y direction) by DFA.

Table 1
The results of scaling exponents by DFA.

	Monthly mean				Daily measured data			
	$k=1$	$k=2$	$k=3$	$k=4$	$k=1$	$k=2$	$k=3$	$k=4$
α	1.0875	1.3581	1.6853	1.8629	1.328	1.4671	1.5005	1.5053

measured data is shown in Fig. 4 with only one order ($k = 1$). Table 1 gives results of scaling exponents.

The analysis from above figures and Table 1 indicates that:

(1) It can be seen from Fig. 3 that the value of log(Fs) decreases on the whole with the increase of the order and each curve tends to be stable gradually at the end of data. All of these plots are mostly close to be straight, have different slopes and are shown for comparison, signifying that the studied time series can be regarded as multifractal measures. From Table 1, the scaling exponent α obtained corresponding to different orders is the curve slope which increases gradually as the order increases but the amplitude of gradual increase is decreasing for. It is needed to point out that log(Fs)~log(s) curves of daily measured data not given except $k = 1$. This is because that it cannot be distinguished well at different orders in the figure due to the large amount of log(Fs) obtained depending on daily measured data, the general trends of other orders are the same as that of $k = 1$. It can also be seen from Table 1 that ranges of scaling exponents corresponding to daily measured time series for different orders are relatively less than those of monthly mean series. According to the principle of DFA, main function of the k-order polynomial fitting is to eliminate k-order tendency fluctuation from accumulative sequence, in other words, to eliminate k-1-order tendency fluctuation from original sequence. Therefore, the greater the sequence fluctuation is, the greater the scaling exponent fluctuation obtained

Table 2
The results of scaling exponents for the monthly mean by MF-DFA.

$H(q)$	Monthly mean				$H'(q)$	Daily measured data				$\acute{H}(q)$
q	$k=1$	2	3	4	$k=3$	$k=1$	2	3	4	$k=3$
−10	1.552	2.222	2.473	3.812	2.749	1.867	1.820	1.840	1.873	1.596
−9	1.549	2.216	2.460	3.801	2.730	1.856	1.811	1.830	1.863	1.590
−8	1.545	2.207	2.444	3.787	2.706	1.843	1.799	1.818	1.852	1.582
−7	1.539	2.196	2.423	3.769	2.675	1.826	1.785	1.803	1.837	1.574
−6	1.531	2.180	2.394	3.742	2.633	1.804	1.767	1.786	1.820	1.564
−5	1.519	2.157	2.353	3.703	2.578	1.775	1.744	1.763	1.798	1.553
−4	1.500	2.120	2.297	3.638	2.504	1.736	1.716	1.736	1.771	1.541
−3	1.471	2.061	2.217	3.522	2.405	1.683	1.680	1.704	1.738	1.526
−2	1.425	1.968	2.110	3.277	2.277	1.616	1.640	1.668	1.698	1.510
−1	1.356	1.836	1.982	2.743	2.129	1.540	1.599	1.630	1.650	1.496
0	1.267	1.672	1.858	2.179	1.979	1.464	1.559	1.590	1.603	1.490
1	1.172	1.502	1.757	1.956	1.839	1.394	1.515	1.547	1.555	1.485
2	1.088	1.358	1.685	1.863	1.715	1.328	1.467	1.501	1.505	1.478
3	1.021	1.253	1.638	1.808	1.615	1.269	1.419	1.455	1.458	1.469
4	0.970	1.179	1.607	1.772	1.540	1.221	1.378	1.418	1.418	1.459
5	0.931	1.127	1.585	1.746	1.485	1.183	1.347	1.388	1.386	1.449
6	0.901	1.091	1.570	1.727	1.445	1.153	1.322	1.366	1.363	1.439
7	0.877	1.063	1.557	1.712	1.416	1.130	1.303	1.348	1.344	1.430
8	0.858	1.043	1.548	1.701	1.394	1.112	1.289	1.335	1.330	1.422
9	0.842	1.027	1.540	1.692	1.377	1.097	1.277	1.324	1.318	1.415
10	0.830	1.014	1.533	1.685	1.364	1.085	1.267	1.315	1.308	1.409

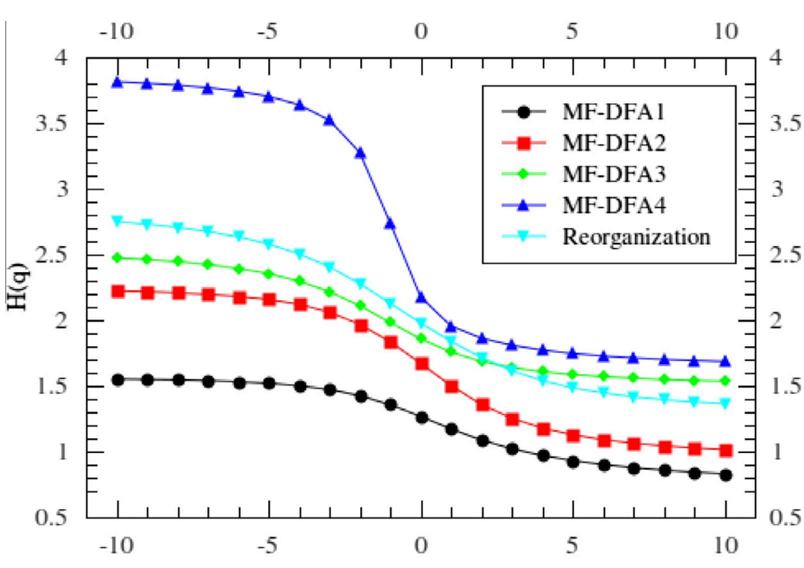

Fig. 5. Analysis results of the monthly mean by MF-DFA.

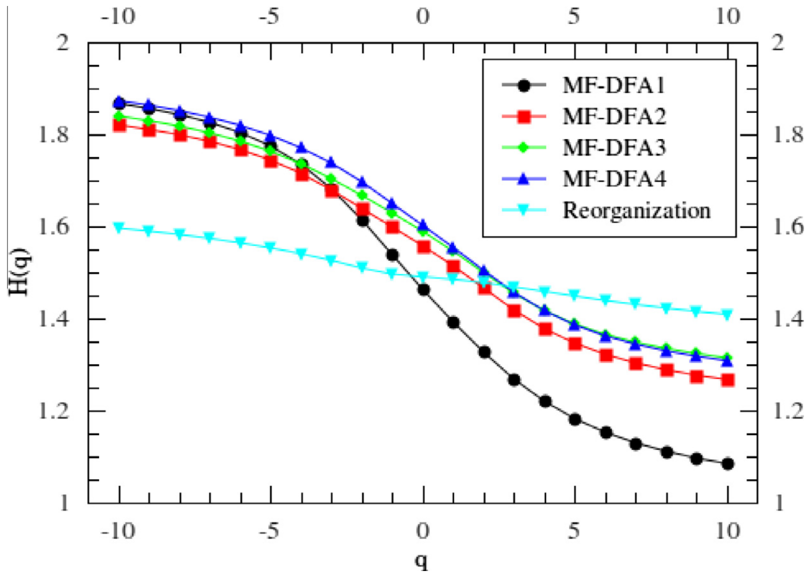

Fig. 6. Analysis results of the daily measured data by MF-DFA.

from this is. The fact, namely the range of daily measured value series is smaller than monthly mean series for different values of k, also reflects the characteristics of monthly mean.

(2) It can be seen from Table 1 that all scaling exponents that are greater than 1.0. The time series of dam displacement exhibits not only long-range correlations but also complex non-power-law correlations. This indicates that displacement series has complex fractal structure and the factors affecting displacement fluctuations are more complex. The scaling exponent of daily measured series which tends to 1.5 means that displacement sequence is similar to the correlation of Brown noise.

(3) The advantages of DFA which can be seen as a conventional analysis method of time series are that DFA can not only analyze potential self-similarity of series but also eliminate spurious correlations caused by strong tendency for the time series which is not determined but looks like an unsteady one.

4.2. Multifractal analysis of dam's displacement time series

The MF-DFA is respectively employed to the time series of daily observation data ($N = 2014$) and monthly mean ($N = 72$) of Y-direction displacement measured by PL4 installed in Block 4#.

As mentioned in Section 3.1, if $|q| \gg 10$, fluctuation functions for $q > 0$ and $q < 0$ correspond to the scaling behavior of large and small fluctuations of displacement time series, respectively. That's to say, the values of q are very important, and the bigger q takes the better for analysis in theory. However the computational complexity doubles with the increase of q, especially when the value of q exceeds a certain limit value increase has almost no effect on the results. Meanwhile, small value range of q can not reflect the fractal features well. According to references(de Moura et al., 2009; Kantelhardt et al., 2002; Telesca et al., 2012a; Telesca et al., 2012b), fractal spectrums are calculated for q in the range $-10 \leqslant q \leqslant 10$.

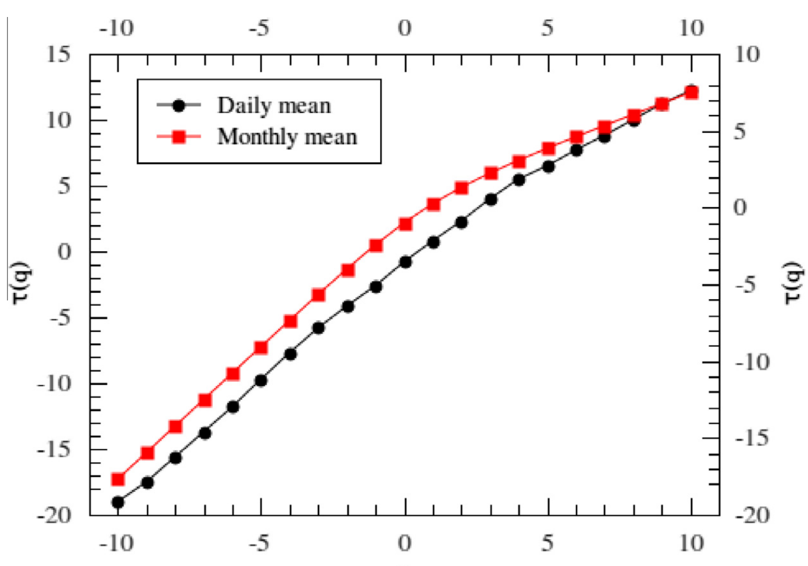

Fig. 7. Relation plots between Renyi index $\tau(q)$ and q for monthly mean and daily measured data.

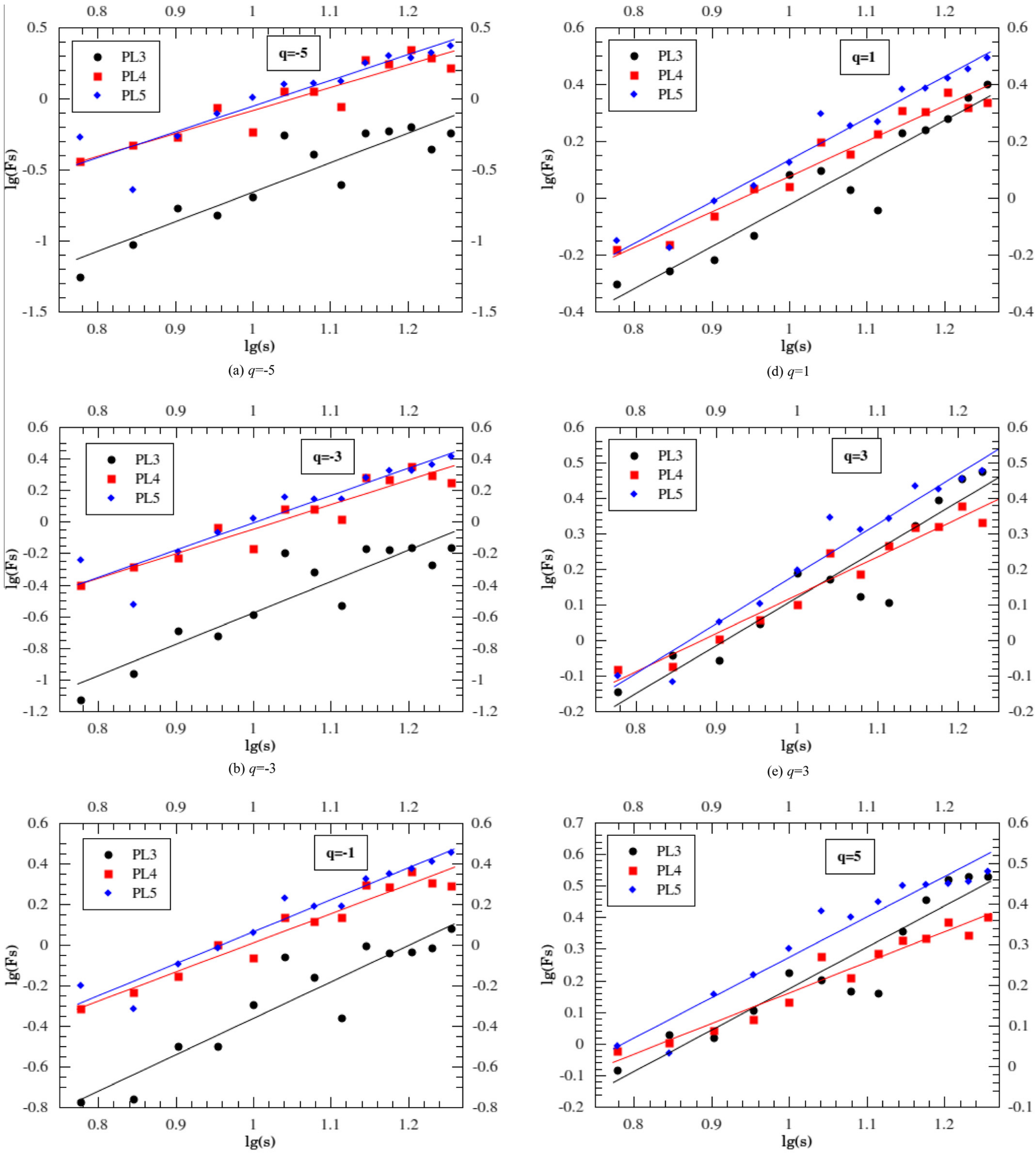

(a) q=-5 (d) q=1
(b) q=-3 (e) q=3
(c) q=-1 (f) q=5

Fig. 8. Analysis results of the monthly mean for measured data of Suspended Pendulums PL3∼5 (Y direction) by DFA.

$\acute{H}(q)$ in the Table 2 which gives the multifractal analysis results is the analysis results after time series reorganization (generating surrogate time series). Time series reorganization is realized by Fourier Transform with the same mean and variance of original one. Changed but uncorrleted phases are assigned randomly to the Fourier transformed time series. Therefore new time series after reorganization has no memory. It is unreasonable for the fractal analysis of displacement time series if the data after reorganization have the same fractal results with original data; the analysis of long-range correlations for time series is credible if the data after reorganization and original data have significantly different analysis results. Figs. 5 and 6 show the relationship between $H(q)$ and q by using MF-DFA to analyze monthly mean and daily measured values respectively. It can be seen from the above figures and tables:

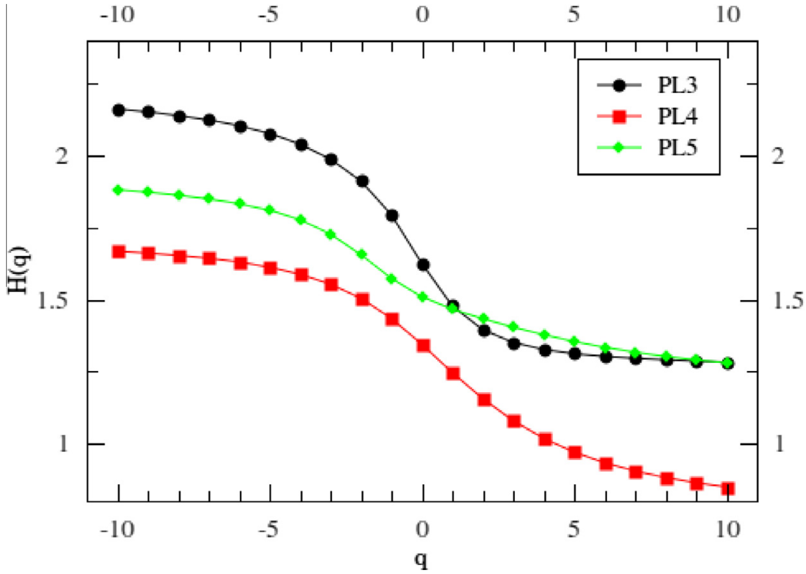

Fig. 9. The q-order $H(q)$ for three time series of PLs3∼5 (Y direction).

(1) The case that $H(q)$ obtained from the analysis of monthly mean and daily measured value are over 1.0 indicates displacement time series has obvious long-range correlations.
(2) For fixed order k, $H(q)$ of the time series of displacement changes with q but not a constant. Both monthly mean and daily measured time series present similar nonlinear relationship between $H(q)$ and q, namely the growing q leads to a decreasing $H(q)$. This indicates that displacement time series has different degree of multifractal features as expected, thus monofractality cannot describe the fluctuation characteristics of displacement well.
(3) From Fig. 5, the values of MF-DFA2 and MF-DFA3 are very close if $q < 0$; the values of MF-DFA3 and MF-DFA4 are very close and the whole range of MF-DFA3 is smaller that tends to 1.5 gradually at the end if $q > 0$. So selecting 3-order polynomial fitting is credible for the monthly mean analysis of displacement sequence. The same to Fig. 6, the values of MF-DFA2 and MF-DFA3 are very close if $q < 0$; the values of MF-DFA3 and MF-DFA4 are very close and the whole range of MF-DFA3 is also smaller that tends to 1.3 gradually at the end if $q > 0$. So selecting 3-order polynomial fitting is credible for the daily measured value analysis of displacement sequence.
(4) Changes of $H(q)$ mainly depend on the variance of small fluctuation if $q < 0$ and changes of $H(q)$ mainly depend on the variance of big fluctuation if $q > 0$. The case that the range of monthly mean and daily measured value are both smaller if $q > 0$ indicates that the whole changes of displacement measured value sequence are smaller and do not have bigger fluctuation.
(5) When the value of q is fixed, the higher the order is, the greater the value of $H(q)$ is. Even if the polynomials of different orders are used, the abilities of eliminating tendency fluctuation are not the same. So the greater the fluctuation of displacement sequence is, the greater the difference of $H(q)$ obtained from different orders is. It can be seen from the figures that $H(q)$ of monthly mean changes greater than daily measured value for the same order and the whole

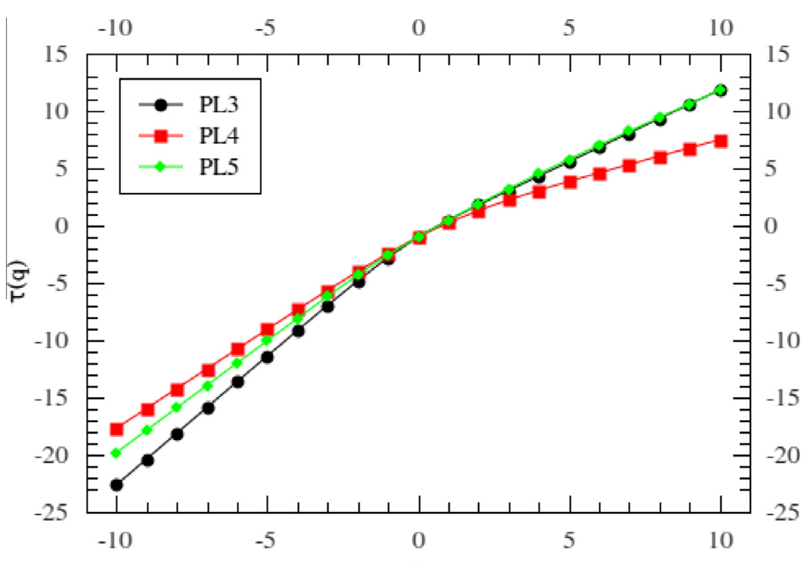

Fig. 10. Renyi index $\tau(q)$ for three time series of PLs3∼5 (Y direction).

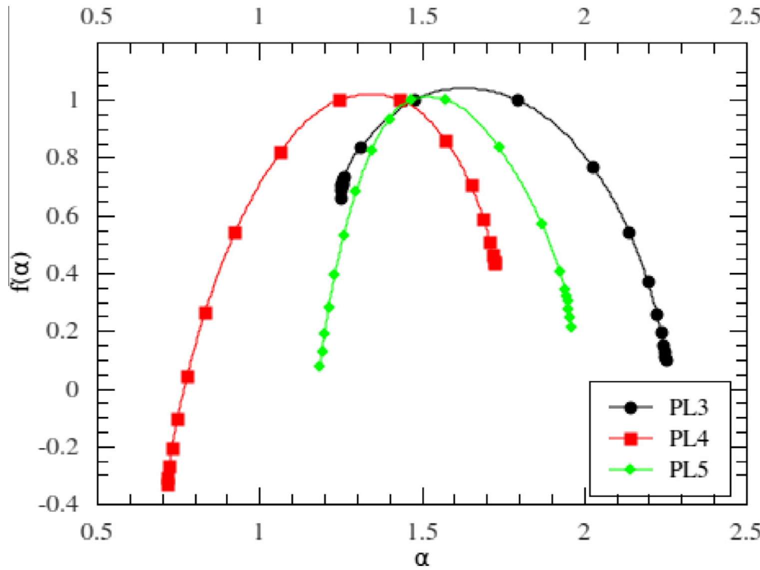

Fig. 11. Multifractal spectrums $f(\alpha)$ for three time series of PLs3∼5 (Y direction).

range of $H(q)$ of daily measured value is much smaller than $H(q)$ of monthly mean. The range of daily measured value for the same order is very small if $q > 2$. So this is in accord with reality that the fluctuation degree of daily measured value is smaller than the fluctuation degree of monthly mean.

(6) According to the analysis conclusion of (3), this paper selects 3-order polynomial fitting to make the same analysis for the sequence after phase reorganization and the analysis results are given in $H'(q)$ column of Table 2. A striking contrast existing between the analysis results after and before reorganization by comparing indicates that the long-range correlations of displacement time series analyzed is not accidental. So it is necessary for the displacement sequence of complex causes to use multifractal analysis method to analyze.

(7) Fig. 7 is the relation graphs between Renyi index $\tau(q)$ and q. It can be seen from the figures that the slope of $\tau(q)$ changes greatly when $q < 0$ and $q > 0$ and $\tau(q)$ is nonlinear obviously. The significant nonlinearity of $\tau(q)$ fully demonstrates multifractal features of displacement time series.

4.3. Multifractal analysis of dam global behavior

As mentioned above, multifractal features exist in the displacement time series of the dam. Next, multifractal analysis of time series of PL3 and PL5 are conducted to compare with that of PL4 to reflect the long term behavior and structural evolution law of the global dam system, and MF-DFA1 has been employed.

To determine the scaling behavior of the fluctuation functions, log–log plots of Fs versus s for time series of all three suspended pendulums are shown in Fig. 8(a)–(f) for several q values (±5,±3,±1) with $k = 1$. Fig. 9 shows the corresponding calculated $H(q)$∼q for three time series using MF-DFA1.

From Fig. 9, $H(q)$ is q dependent for these time series. In other words, multifractal characteristics really exist in deformation fluctuation series. Since this, the deformation fluctuation series may be transferred into a more useful compact form through the multifractal formalism, namely, the $f(\alpha)$∼α plots. Fig. 10 shows plots of mass exponents Renyi index $\tau(q)$ versus q for three time series with MF-DFA1, and Fig. 11 shows the corresponding $f(\alpha)$ spectrums calculated from $H(q)$ using Legendre transform namely Eq. (20).

It can be seen from the above figures:

(1) The results of Fs∼s for three time series are compared in Fig. 8(a)–(f). The small segments are able to distinguish between the local periods with large and small fluctuations (i.e., positive and negative q's, respectively) because the small segments are embedded within these periods. In contrast, the large segments cross several local periods with both small and large fluctuations and will therefore average out their differences in magnitude. From Fig. 2, it is observed that time series of PL4 and PL5 fluctuate with the same trend and magnitude among these years. As shown in Fig. 8(a)–(f), nice agreement is observed for Fs∼s plots of time series of PL4 and PL5 especially around lower values of q.

(2) Only if small and large fluctuations scale differently, there will be a significant dependence of $H(q)$ on q. For positive values of q, $H(q)$ describes the scaling behavior of the segments with large fluctuations, on the contrary, for negative values of q, $H(q)$ describes the scaling behavior of the segments with small fluctuations. Usually large fluctuations are characterized by a smaller scaling exponent $H(q)$ for multifractal series than the small fluctuations. In Fig. 9, variation trends of $H(q)$∼q plots accord well with each other. However, it is also found that some small differences exist. These can be boiled down to differences caused by the large and small fluctuations. The results are in good agreement with general law, showing that the MF-DFA correctly detects the multifractal scaling exponents of dam deformation.

(3) Fig. 10 shows that three time series have mass exponents Renyi index $\tau(q)$ with a curved q-dependecny The resulting multifractal spectrum is where the difference between the maximum and minimum α are called the width of multifractal spectrum $\Delta\alpha$ ($\alpha_{max} - \alpha_{min}$). The higher the range (width) $\Delta\alpha$, the higher the multifractal degree.$\Delta\alpha$ may indicate absolute magnitudes of deformations in a dam, larger the value of $\Delta\alpha$, weaker the local or dam block. Different fluctuation scopes and movement trends correspond to multifractal spectra with different sizes and shapes (i.e., a hook to the left as PL3 and a hook to the right as PL4). Meanwhile, the Δf may indicate the different trends of deformation movements. Values of $\Delta\alpha$ of PL3∼PL5 are respectively equal to 1.0033, 1.0086 and 0.7727. This can also be found from Fig. 11. These figures and data indicate that Block 5 has the most normal deformation fluctuations according with

environmental factors (i.e., water pressure, rain and air temperature etc.). On the contrary, time series of PL3 and 4 show more multifractal characteristics. Intuitively, the multifractal spectra may contain some useful statistical information about the deformation movements of dams.

5. Conclusions

The physical phenomenon underlying the observed time series is complex. The use of multifractal methods in investigating the spatiotemporal fluctuations of the observed time series can lead to a better understanding of such complexity. The determination of the multifractality has been performed by means of the MF-DFA method, which has revealed a clear multifractal characteristic of the time series, mostly due to different long-range correlations for small and large fluctuations.

(1) The DFA was used to analyze the monofractal scaling properties of the *in situ* time series of dam. The results indicate that this time series has obvious fractal features and typical long-range correlation.
(2) According to the time dependent characteristics appear in observed time series of dam, the framework for analyzing multifractals based on MF-DFA was proposed. Time series of deformation observed from one existing gravity dam was investigated. The time series exhibits not a simple monofractal scaling behavior but multifractal characteristics. The scaling behavior in the observed time series of dam is so complicated that different scaling exponents are required for different parts of the series. The MF-DFA based method can depict the fractal features with different time scales especially smaller scales, namely a full description of the scaling behavior.
(3) Monofractal in time series identifies the long range statistical characteristics of long term dam behavior, thus in the sense this exponent only describes the fluctuations for the original series in one large scale. In this case monofractal doesn't take different parts of the series into account. Multifractals observed in deformation time series reflect the irregularity and singularity, within which phenomena internal or external influencing factors vary. In other words, the structure of the time series is linked to the structural behavior under corresponding environments. Multifractals within different small scales can better depict the underlying behavior evolution.
(4) Since the observation of multifractal spectrum of deformation fluctuation in dam monitoring system has led to a better understanding of such complexity, this should be encouraged.
(5) The determination of the multifractality has been performed by means of the MF-DFA method, which has revealed clear multifractal characteristics of the time series, mostly due to different long-range correlations for small and large fluctuations. The potential of multifractal analysis is far from being fully exploited, in our future work the variation of the multifractal of the time series should also be investigated in a more systemic way, namely not only the consequences but also the influencing factor should be understood in depth.

Acknowledgements

This research has been partially supported by National Natural Science Foundation of China (SN: 51179066, 51139001), Jiangsu Natural Science Foundation (SN: BK2012036), the Program for New Century Excellent Talents in University (SN: NCET-10-0359), Jiangsu Province "333 High-Level Personnel Training Project" (SN: BRA2011179), Non-profit Industry Financial Program of MWR (SN: 201301061, 201201038) and Open Foundation of State Key Laboratory of Hydrology-Water Resources and Hydraulic Engineering (SN: 2012490211).

References

Alvarez-Ramirez, J., Rodriguez, E., & Echeverria, J. C. (2009). A DFA approach for assessing asymmetric correlations. *Physica A: Statistical Mechanics and its Applications, 388*(12), 2263–2270.
Barabasi, A. L., & Vicsek, T. (1991). Multifractality of self-affine fractals. *Physical Review A, 44*(4), 2730–2733.
Bernaola-Galván, P., Ivanov, P. C., Nunes Amaral, L. A., & Eugene Stanley, H. (2001). Scale invariance in the nonstationarity of human heart rate. *Physical Review Letters, 87*(16), 168105.
Coniglio, A., de Arcangelis, L., & Herrmann, H. J. (1989). Fractals and multifractals: Applications in physics. *Physica A, 157*, 21–30.
de Moura, E. P., Vieira, A. P., Irmao, M. A. S., & Silva, A. A. (2009). Applications of detrended-fluctuation analysis to gearbox fault diagnosis. *Mechanical Systems and Signal Processing, 23*(3), 682–689.
Foufoula-Georgiou, E., & Sapozhnikov, V. (2001). Scale invariances in the morphology and evolution of braided rivers. *International Association for Mathematical Geology, 33*(3), 273–291.
Govindan, R. B., Wilson, J. D., Preißl, H., Eswaran, H., Campbell, J. Q., & Lowery, C. L. (2007). Detrended fluctuation analysis of short datasets: An application to fetal cardiac data. *Physica D: Nonlinear Phenomena, 226*(1), 23–31.
Halsey, T. C., Jensen, M. H., Kadanoff, L. P., Procaccia, I., & Shraiman, B. I. (1986). Fractal measures and their singularities: The characterization of strange sets. *Physical Review A, 33*(2), 1141–1151.
Huang, Z.-W., Liu, C.-Q., Shi, K., & Zhang, B. (2010). Monofractal and multifractal scaling analysis of pH time series from Dongting lake inlet and outlet. *Fractals, 18*(3), 309–317.
Kantelhardt, J. W., Koscielny-Bunde, E., Rego, H. H. A., Havlin, S., & Bunde, A. (2001). Detecting long-range correlations with detrended fluctuation analysis. *Physica A, 295*, 441–454.
Kantelhardt, J. W., Zschiegner, S. A., Koscielny-Bunde, E., Havlin, S., Bunde, A., & Eugene Stanley, H. (2002). Multifractal detrended fluctuation analysis of nonstationary time series. *Physica A, 316*(87), 87–114.
Kawada, Y., Nagahama, H., & Nakamura, N. (2007). Time-scale invariances in preseismic electromagnetic radiation, magnetization and damage evolution of rocks. *Natural Hazards and Earth System Sciences, 7*(5), 599–606.
Lau, K. S., & Ngai, S. M. (1999). Multifractal measures and a weak separation condition. *Advances in Mathematics, 141*(1), 45–96.
Liu, X., Wu, Z. R., Yang, Y., & Hu, J. (2012). Information fusion diagnosis and early-warning method for monitoring the long-term service safety of high dams. *Journal of Zhejiang University-SCIENCE A (Applied Physics & Engineering), 13*(9), 687–699.
Loh, C. H., Chen, C. H., & Hsu, T. Y. (2011). Application of advanced statistical methods for extracting long-term trends in static monitoring data from an arch dam. *Structural Health Monitoring, 10*(6), 587–601.
Longley, P. A., & Batty, M. (1989). Fractal measurement and line generalization. *Computers & Geosciences, 15*(2), 167–183.
Niu, M. R., Wang, F. C., Liang, Q. F., Yu, G. S., & Yu, Z. H. (2008). Multifractal detrended fluctuation analysis of pressure fluctuation signals in an impinging entrained-flow gasifier. *Chemical Engineering Journal, 136*(2–3), 364–372.
Peng, C. K., Buldyrev, S. V., Havlin, S. S., et al. (1994). Mosaic organization of DNA nucleotides. *Physical Review E, 49*(2), 1685–1689.
Su, H. Z., Hu, J., & Wu, Z. R. (2012). A study of safety evaluation and early-warning method for dam global behavior. *Structural Health Monitoring, 11*(3), 269–279.
Telesca, L., Colangelo, G., Lapenna, V., & Macchiato, M. (2004). Fluctuation dynamics in geoelectrical data: An investigation by using multifractal detrended fluctuation analysis. *Physics Letters A, 332*(5–6), 398–404.
Telesca, L., & Lovallo, M. (2011). Analysis of time dynamics in wind records by means of multifractal detrended fluctuation analysis and Fisher–Shannon information plane. *Journal of Statistical Mechanics: Theory and Experiment*, P07001.
Telesca, L., Lovallo, M., Hsu, H.-L., & Chen, C.-C. (2012). Analysis of site effects in magnetotelluric data by using the multifractal detrended fluctuation analysis. *Journal of Asian Earth Science, 54–55*, 72–77.
Telesca, L., Lovallo, M., Lopez-Moreno, I., & Vicente-Serrano, S. (2012a). Investigation of scaling properties in monthly streamflow and Standardized Streamflow Index (SSI) time series in the Ebro basin (Spain). *Physica A, 391*, 1662–1678.
Telesca, L., Pierini, J. O., & Scian, B. (2012b). Investigating the temporal variation of the scaling behavior in rainfall data measured in central Argentina by means of the detrended fluctuation analysis. *Physica A, 391*, 1553–1562.